analytical chemistry

Article

pubs.acs.org/ac

Multiplexed Fluorescence Resonance Energy Transfer Aptasensor between Upconversion Nanoparticles and Graphene Oxide for the Simultaneous Determination of Mycotoxins

Shijia Wu,[†] Nuo Duan,[†] Xiaoyuan Ma,[†] Yu Xia,[†] Hongxin Wang,[†] Zhouping Wang,*[,†] and Qian Zhang*[,‡]

[†]State Key Laboratory of Food Science and Technology, School of Food Science and Technology, Jiangnan University, Wuxi, Jiangsu, 214122, P. R. China

[‡]College of Chemistry, Liaoning University, Shenyang, Liaoning, 110036, P. R. China

Supporting Information

ABSTRACT: We presented a new aptasensor for mycotoxins, which was based on multiplexed fluorescence resonance energy transfer (FRET) between multicolor upconversion fluorescent nanoparticles (UCNPs) as donors and graphene oxide (GO) as the entire and effective acceptor. $BaY_{0.78}F_5$:$Yb_{0.2}$, $Er_{0.02}$ and $BaY_{0.78}F_5$:$Yb_{0.7}$, $Tm_{0.02}$ upconversion nanoparticles were synthesized and functionalized, respectively, with immobilized ochratoxin A (OTA)-aptamers and fumonisin B_1 (FB_1)-aptamers. On the basis of the strong $\pi-\pi$ stacking effect between the nucleobases of the aptamers and the sp^2 atoms of GO, the aptamer modified-UCNPs can be brought in close proximity to the GO surface. The strong upconversion fluorescence both of $BaY_{0.78}F_5$:$Yb_{0.2}$, $Er_{0.02}$ and $BaY_{0.78}F_5$:$Yb_{0.2}$, $Tm_{0.02}$ can be completely quenched by the GO, because of a good overlap between the fluorescence emission of multicolor UCNPs and the absorption spectrum of GO. In contrast, in the presence of OTA and FB_1, the aptamers preferred to bind to their corresponding mycotoxins, which led to changes in the formation of aptamers, and therefore, aptamer modified-UCNPs were far away from the GO surface. Our study results showed that the fluorescence intensity of $BaYF_5$:Yb Er and $BaYF_5$:Yb Tm were related to the concentration of OTA and FB_1. We therefore developed a sensitive and simple platform for the simultaneous detection of OTA and FB_1 with multicolor UCNPs and GO as the FRET pair. The aptasensor provided a linear range from 0.05 to 100 ng·mL^{-1} for OTA and 0.1 to 500 ng·mL^{-1} for FB_1; the detection limit of OTA was 0.02 ng·mL^{-1} and FB_1 was 0.1 ng·mL^{-1}. As a practical application, the aptasensor was used to monitor OTA and FB_1 level in naturally contaminated maize samples with the results consistent with that of a classic ELISA method. More importantly, the novel multiplexed FRET was established for the first time based on multiplexed energy donors to the entire energy acceptor; this work was expected to open up a new field of FRET system applications for various targets.

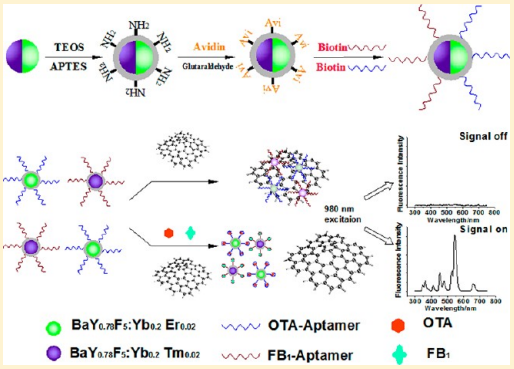

Fluorescence resonance energy transfer (FRET) is a typical homogeneous assay technique that is based on the transfer of nonradiative energy from donors to acceptors that are in close proximity to each other (normally 1−10 nm), via long-range dipole−dipole interactions.[1] In a well-designed FRET model, the donors and acceptors are brought to a proper distance from each other exclusively through the recognition of target substances. FRET-based assays, therefore, typically show pronounced specificity. In combination with the high sensitivity of fluorescence, FRET has been recognized as an exceptionally sensitive method and has been widely used in bioassays.[2,3] In addition, the energy transfer efficiency between a selected donor−acceptor pair is an important consideration because it is the determining factor for detection sensitivity. At present, most of researchers focus their attention on finding the perfect donor−acceptor pair to improve FRET efficiency. These energy donors include organic fluorescent dyes, semiconductor quantum dots, and upconversion fluorescence nanoparticles (UCNPs), while energy acceptors include organic quenchers, gold nanoparticles, and graphene. Among these fluorescent materials, UCNPs have significant advantages over traditional organic fluorophores due to their attractive optical and chemical features, which would not be absorbed by biological samples and induces no autofluorescence and light scattering background. As a result, the signal-to-background ratio and the resistance to photobleaching and blinking can be greatly improved with UCNPs. Therefore, UCNPs are widely used as novel fluorescent labels recently. In fact, these advantages make UCNPs an ideal choice as the donor in the FRET-based turn-on assay. The earliest reports on FRET using UCNPs as energy donors appeared in 2005,[4] with gold nanoparticles being employed as UCNPs quenchers, and after this, the FRET system between UCNPs and fluorescent dye or quantum dots

Received: June 8, 2012
Accepted: June 25, 2012
Published: June 25, 2012

   dx.doi.org/10.1021/ac301534w | *Anal. Chem.* 2012, 84, 6263−6270

were developed for in vivo studies.[5,6] Additionally, the interesting physical properties of graphene, a novel one-atom-thick two-dimensional graphitic carbon system, have led to a great deal of excitement in recent years in material science and condensed-matter physics. In fact, several reports about fluorescent sensing using graphene as a fluorescence quencher[7,8] have been published. Moreover, both Liu's group[9] and Li's group[10] have employed UCNPs-graphene (or graphene oxide) as the donor−acceptor pair to develop a sensitive FRET-based assay to detect some significant molecules, such as adenosine triphosphate and glucose.

To date, few reports in the literature address whether various types of fluorescent donors can be quenched by the same kind of acceptors simultaneously. We therefore developed an analytical method based on multiplexed-FRET. UCNPs-graphene oxide was chosen as a donor−acceptor FRET pair due to the tunable optical properties of the UCNPs (by varying the lanthanide dopants, e.g., Tm, Er, Ho), the host matrix used in their synthesis. On the basis of multicolor fine-tuning and zero overlap in the visible spectral region, UCNPs can be applied as donors to simultaneous, multiplexed-FRET. More importantly, the absorption spectrum of graphene oxide spans a wide range of wavelengths (approximately 300−700 nm), overlapping the fluorescence spectra of various fluorescent materials, including the UCNPs doped with Er and Tm. This remarkable property helps graphene to play an indispensable role in the system of multiplexed FRET.

Mycotoxins are a group of chemical substances produced by some fungal species and can cause illness or even death. A wide range of methods are currently available, including instrumental analytical methods,[11−15] but they are time-consuming and require complex sample preparation and expensive equipment. Biosensors are considered to be very good alternative techniques for the detection of low-molecular weight compounds such as toxins.[16−21] Among the above detections, the methods based on optical biosensors are impressive. However, it is seldom for the simultaneous and sensitive determinations of mycotoxins using multicolor fluorescent nanoparticles. For a long time, our research group has developed the detection of mycotoxins using multicolor-UCNPs as labels.[22] According to our knowledge, there have been few reports on the use of FRET for the simultaneous determination of mycotoxins; the reason may be that the system of multiplexed FRET is not mentioned.

Therefore, a unique aspect of our work is that we first developed a multiplexed FRET-based turn-on assay for the simultaneous detection of two types of mycotonxins. Ochratoxin A (OTA) and fumonisin B_1 (FB_1) are selected as proof-of-concept targets in this study while the aptamers of OTA and FB_1 are designed as mentioned. Multicolor UCNPs doped with Er and Tm are synthesized as donors together with graphene oxide (GO) as the entire and effective acceptor. This work is expected to open up a new field of FRET system applications.

MATERIALS AND METHODS

Materials and Instrumentation. Rare-earth oxides used in this work, including yttrium oxide (Y_2O_3), ytterbium oxide (Yb_2O_3), and erbium oxide (Er_2O_3), were of 99.99% purity. Barium nitrate ($Ba(NO_3)_2$), sodium fluoborate ($NaBF_4$), 25% ammonia ($NH_3{\cdot}H_2O$), sodium hydroxide (NaOH), nitric acid (HNO_3), ethylene diamine tetraacetic acid (EDTA), 25% glutaraldehyde ($OHC(CH_2)_3CHO$), and tetraethyl orthosilicate (TEOS) were of analytical grade. All the chemicals above were purchased from Sinopharm Chemical Reagent Co., Ltd. (Shanghai, China). 3-Aminopropyltrimethoxysilane (APTES; 98%) was purchased from Alfa Aesar (USA). The sequence of Fumonisin B_1 aptamer was 5′-biotin-$(CH_2)_6$-ATA CCA GCT TAT TCA ATT AAT CGC ATT ACC TTA TAC CAG CTT ATT CAA TTA CGT CTG CAC ATA CCA GCT TAT TCA ATT AGA TAG TAA GTG CAA TCT-3′ (reported by Maureen McKeague and Maria C. DeRosa),[23] and the sequence of OTA aptamer was 5′-GAT CGG GTG TGG GTG GCG TAA AGG GAG CAT CGG-$(CH_2)_6$-biotin-3′ (reported by Cruz-Aguado and Penner)[24] synthesized by Shanghai Sangon Biological Science & Technology Company (Shanghai, China). The size and morphology of nanoparticles were determined using a JEM-2100HR transmission electron microscope (TEM, JEOL Ltd., Japan). X-ray diffraction (XRD) measurements were performed using a D8-advance instrument (Bruker AXS Ltd., Germany). Upconversion fluorescence spectra were measured using an F-7000 fluorescence spectrophotometer (Hitachi Co., Japan) modified with an external 980 nm laser (Beijing Hi-Tech Optoelectronic Co., China) instead of the internal excitation source. Ultraviolet−visible (UV−vis) absorption spectra were recorded using a Shimadzu UV-2300 UV−vis spectrophotometer (Shimadzu, Japan). FT-IR spectra of the bionanoparticles were obtained with a Nicolet Nexus 470 Fourier transform infrared spectrophotometer (Thermo Electron Co., U.S.A.) using the KBr method. The morphology of the prepared GO was characterized on Dimension 3100 atomic force microscopy (AFM) using the tapping mode.

Synthesis and Surface Modification of $BaYF_5$:Yb Er/Tm Upconversion Nanoparticles. In a typical procedure for the synthesis of $BaY_{0.78}F_5$:$Yb_{0.2}$ $Er_{0.02}$ UCNPs according to the method described by our previous work and Yang's group with slightly modifications,[22,25,26] 0.1761 g (0.78 mmol) of Y_2O_3, 0.0788 g (0.2 mmol) of Yb_2O_3, and 0.0076 g (0.02 mmol) of Er_2O_3 were dissolved in dilute HNO_3 solution with heating and stirring until the superfluous HNO_3 was removed. The obtained rare earth nitrate and 0.5227 g (2 mmol) of $Ba(NO_3)_2$ were dissolved in 20 mL of deionized water. Then, 10 mL of EDTA (2 mmol) solution (molar ratio with RE^{3+} was 2/1) was added slowly into the previous solution with intense stirring for 15 min. After that, 10 mL of solution containing 2.7449 g (25 mmol) of $NaBF_4$ was added dropwise under continuous stirring. The final pH value of the solution was adjusted to 10 with ammonia (25 wt %). After further stirring for 10 min, the as-obtained mixing solution was transferred into a 50 mL Teflon bottle held in a stainless steel autoclave, sealed, and maintained at 180 °C for 24 h. As the autoclave cooled to room temperature naturally, the precipitates were washed with hot water into a beaker, dispersed ultrasonically for 10 min, and allowed to stand for several minutes after which the supernatant was discarded; this process was repeated three times. The UCNPs were purified by centrifugation, washed with ethanol three times, and dried at 60 °C for 12 h to gain the final sample. $BaY_{0.78}F_5$:$Yb_{0.2}$ $Tm_{0.02}$ with the doping concentration of 20 mol % of Yb^{3+} to Y^{3+} and 2 mol % of Tm^{3+} to Y^{3+} were synthesized similarly to the above procedure.

Surface modification of $BaYF_5$:Yb Er/Tm UCNPs were prepared by PVP-assisted cap silica onto the surface of the UCNPs.[27,28] In a 250 mL flask, 100 mg of UCNPs and 60 mg of PVP were dispersed in 60 mL of 3-propanol by sonication and agitation for 40 min, and then, 2.5 mL of ammonia and 20 mL of water were added to the flask; the mixture was

dx.doi.org/10.1021/ac301534w | Anal. Chem. 2012, 84, 6263−6270

Scheme 1. Schematic Illustration of the Multiplexed Upconversion Fluorescence Resonance Energy Transfer between Aptamers-UCNPs and GO for FB_1 and OTA Detection

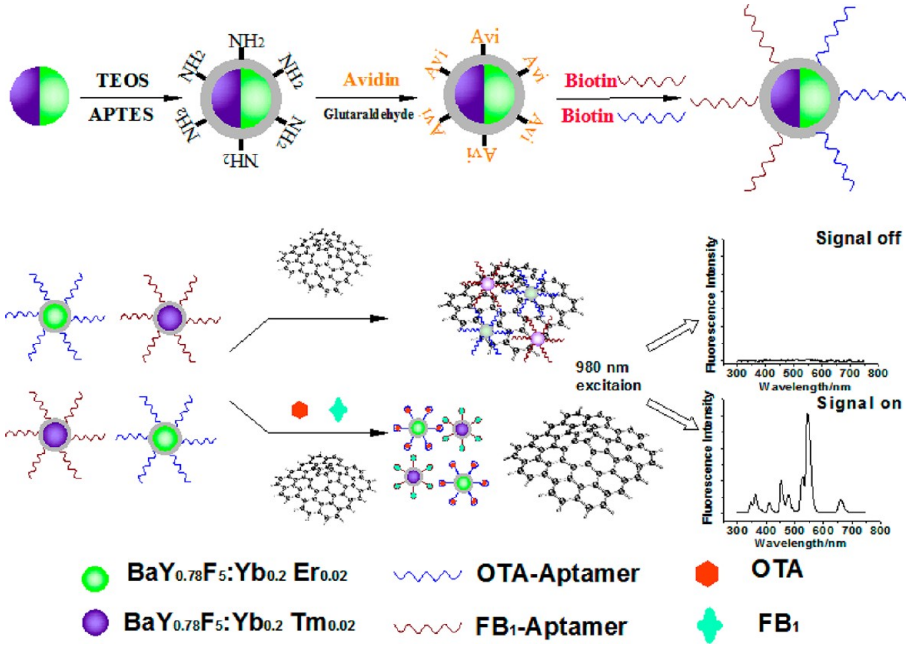

maintained at 35 °C under vigorous stirring. A solution containing 20 mL of 3-propanol and 75 μL of TEOS was added dropwise to the mixture over a period of 1 h, and the reaction was continued for another 3 h. In order to synthesize amino-modified UCNPs, a solution containing 30 mL of 3-propanol and 200 μL of APTES was then added dropwise into the suspension, and the reaction was continued for 1 h. When the reaction terminated, the product was aged for 2 h at room temperature. Then, the precipitates were separated by centrifugation, washed with ethanol three times, and then dried at 60 °C for 12 h to obtain amino-functionalized UCNPs. Amino-modified $BaYF_5$:Yb Er/Tm UCNPs were thus formed.

Amino-modified $BaYF_5$:Yb Er/Tm UCNPs were conjugated with avidin by a classical glutaraldehyde method described by our previously reported approach. Typically, 10 mg of the UCNPs were dispersed in 5 mL of 10 mmol·L^{-1} phosphate buffer solution (PBS) at pH 7.4 by ultrasonication for 15 min, and then 1.25 mL of 25% glutaraldehyde was added into the mixture. The mixture was shaken slowly on a shaking table at room temperature for 2 h; the UCNPs were separated by centrifugation and then washed with phosphate buffer solution three times. Subsequently, the resultant UCNPs were dispersed in 4 mL of 10 mmol·L^{-1} phosphate buffer solution by ultrasonication again, followed by addition of 200 μL of 5.0 mg·mL^{-1} avidin. The mixture was shaken slowly on a shaking table at room temperature for 12 h. The avidin-conjugated UCNPs were separated and washed with PBS three times with the supernatant discarded each time. After final removal of the supernatant, the precipitates were dried at 37 °C for 12 h.

Attachment of Aptamers to Upconversion Nanoparticles. The biotin modified OTA and FB_1 aptamers were linked to avidin-conjugated $BaYF_5$:Yb Er/Tm UCNPs, respectively, through the biotin−avidin affinity reaction. Take the preparation of OTA aptamer modified-$BaYF_5$:Yb Er UCNPs conjugation as an example. Briefly, the $BaYF_5$:Yb Er nanoparticles were derivatized with modified OTA aptamers by incubating ∼2 mg·mL^{-1} of nanoparticle solution overnight with 200 nM of oligonucleotides in Tris-HCl buffer (containing 0.1 M NaCl, pH 7.4) at 37 °C. Following removal of the supernatant, the modified nanoparticles were washed twice with PBS buffer by centrifugation and redispersion and then finally redispersed in fresh PBS buffer. The cross-linking of FB_1 aptamers with $BaYF_5$:Yb Tm UCNPs was performed following the similar procedures.

Synthesis of Graphene Oxide. Graphene oxide (GO) was prepared from graphite powder by a modified Hummer's method.[29] GO was synthesized from graphite powder according to the Hummers method. Briefly, 2 g of powered flake graphite and 1.6 g of $NaNO_3$ were added to 67.5 mL of 98% H_2SO_4 in an ice bath. After that, 9 g of $KMnO_4$ was slowly added to the mixture with stirring. The mixture was then maintained at 35 °C for 30 min. After being kept at room temperature with mechanical stirring for 5 days, 560 mL of warm water was slowly stirred into the paste and further treated with 30% H_2O_2. Upon treatment with the peroxide, the suspension turned bright yellow. The suspension was then centrifuged, washed with distilled water, and air-dried overnight at 70 °C to get GO.

Simultaneous Detection of OTA and FB_1 Based on Multiplexed FRET Assay. A certain concentration of OTA standard solution and OTA aptamer modified-$BaYF_5$:Yb Er and FB_1 standard solution and FB_1 aptamer modified-$BaYF_5$:Yb Tm UCNPs (final concentration of 0.5 mg·mL^{-1}) were mixed in Tris-HCl buffer (10 mM containing 100 mM NaCl, pH 7.4). The mixture was incubated at 37 °C for 2 h. GO (final concentration of 0.6 mg·mL^{-1}) was subsequently added to the mixture and further incubated at 37 °C for 80 min. The upconversion fluorescence spectra of the final mixture were then measured using an F-7000 fluorescence spectrometer with an external 980 nm laser as the excitation source in place of the xenon lamp in the spectrometer.

dx.doi.org/10.1021/ac301534w | Anal. Chem. 2012, 84, 6263−6270

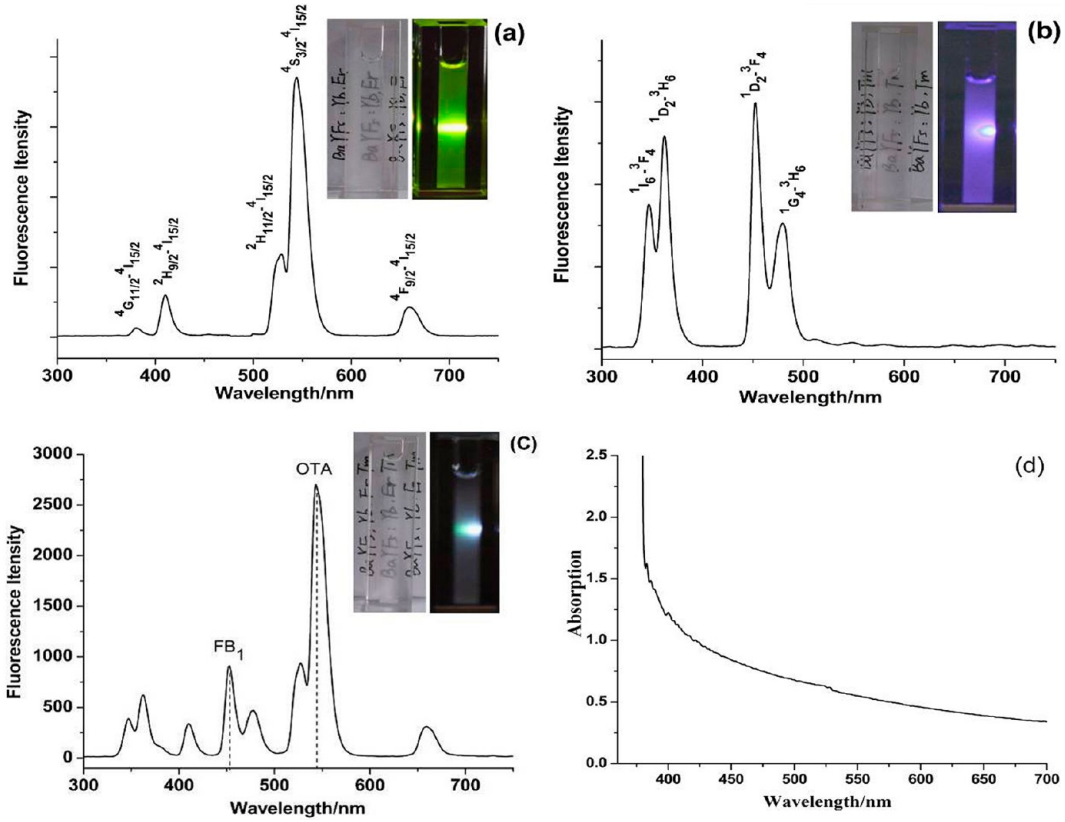

Figure 1. The fluorescence spectra of $BaY_{0.78}F_5$:$Yb_{0.2}$, $Er_{0.02}$ UCNPs (a), $BaY_{0.78}F_5$:$Yb_{0.2}$, $Tm_{0.02}$ UCNPs (b), and the mixture (c). The inset shows a photograph of the naked-eye visible upconversion fluorescence of the $BaY_{0.78}F_5$:$Yb_{0.2}$ $Er_{0.02}$/$Tm_{0.02}$ nanoparticles and of a mixture solution of nanoparticles. All solutions were excited with an external 980 nm laser. Absorption spectrum of as-prepared graphene oxide (d).

RESULTS AND DISCUSSION

Principle of Multiplexed FRET Aptasensor for Mycotoxins. We developed a sensitive platform for the simultaneous detection of OTA and FB_1 with mulitcolor UCNPs and GO as the FRET pair. As shown in Scheme 1, both OTA aptamer modified $BaYF_5$:Yb Er and FB_1 aptamer modified $BaYF_5$:Yb Tm UCNPs exhibit intense upconversion fluorescence at an excitation wavelength of 980 nm. On the basis of the strong $\pi-\pi$ stacking effect between the nucleobases of the aptamers and the sp^2 atoms of GO, the aptamers-UCNPs can be brought in close proximity to the GO surface.[7,9,30,31] Moreover, there is good overlap between the fluorescence emission of multicolor UCNPs and the absorption spectrum of GO (Figure 1). Therefore, the strong upconversion fluorescence can be completely quenched upon the addition of GO. In contrast, in the presence of OTA and FB_1, the aptamers prefer to bind to their corresponding mycotoxins, which leads to changes in the formation of aptamers and therefore decreases the surface charge of the DNA molecules and the exposure of nucleobases.[30,31] As a result, part of the multicolor upconversion fluorescence of aptamer modified UCNPs cannot be quenched because the UCNPs are far away from the GO surface. Our study results showed that the fluorescence intensity of $BaYF_5$:Yb Er and $BaYF_5$:Yb Tm were related to the concentration of OTA and FB_1.

Characterization of $BaYF_5$:Yb Er/Tm Upconversion Nanoparticles. Typically, in upconversion materials, fluorides are efficient hosts due to their photons, which have sufficient energy to produce strong upconversion fluorescence. As an important category of fluorides, $BaYF_5$ is a particularly promising host material that can be doped with divalent or trivalent lanthanide ions, exhibiting a strong broadband emission in the near UV spectra region and a highly efficient infrared to visible UC light at the submicrometer-nano scale.[32,33] In the bulk state, it is reported that $BaYF_5$:Yb Er/Tm is an excellent upconversion material. In Yb^{3+} and Er^{3+} codoped systems (Figure 1a), Yb^{3+} ions act as sensitizers while Er^{3+} ions act as activators. Four groups emission lines appear, peaking at 410, 525, 544, and 660 nm. In Yb^{3+} and Tm^{3+} codoped systems (Figure 1b), four groups of emission lines appear, with maxima at 347, 362, 452, and 477 nm. More importantly, the emission peaks of $BaYF_5$:Yb Er/Tm do not overlap and can be clearly distinguished from each other (Figure 1c). It is essential for establishment of a multiplexed FRET system.

Tetragonal $BaYF_5$ UCNPs with a spherical morphology and an average diameter of ~30 nm have been successfully synthesized via a facile and effective hydrothermal route in water medium (Figure S1a, Supporting Information). After surface modification by SiO_2, the size of the UCNPs increased to approximately 35 nm due to the formation of a 5 nm-thick silica layer on the surface of the bare UCNPs (Figure S1b, Supporting Information). The crystal structure and phase purity of the resulting product were examined by X-ray powder diffraction. Figure S2 (Supporting Information) shows the XRD patterns of the as-synthesized $BaYF_5$:Yb/Ln (Ln = Er, Tm) NPs. All of the samples exhibit the peaks of pure crystalline tetragonal $BaYF_5$, which are consistent with the standard data (JCPDS No. 46-0039). For biological labeling applications, UCNPs should not only exhibit high upconversion

dx.doi.org/10.1021/ac301534w | Anal. Chem. 2012, 84, 6263−6270

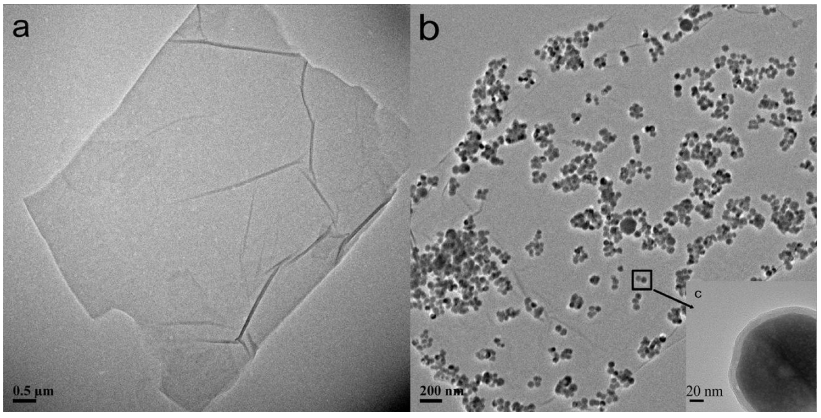

Figure 2. High resolution TEM image of graphene oxide (a) and complex of graphene oxide and UCNPs (b) (inset: the TEM image of that black box indicated at higher magnification). The concentration of GO was 0.2 mg·mL^{-1}.

flourescent efficiency but also have surface wetting characteristics that are compatible with biomolecules or biomolecular assemblies such as nucleic acids. Thus, the UCNPs were first coated with a silica shell and then further functionalized with APTES to form an amino-terminated surface via a typical Stöber-based modification method. The resulting amino-functionalized $BaYF_5$:Yb Er/Tm UCNPs could be easily dispersed in water to form a colloidal solution. The functional groups on the surfaces of the amino-modified UCNPs were identified by FT-IR (Figure S2, Supporting Information). A strong transmission band in the approximate region of 1066 cm^{-1} can be attributed to the symmetrical stretching vibration of the Si−O bond, suggesting that the UCNPs are coated with a layer of silica. The stretching and bending vibration bands of the amine group appear at 3421 and 1648 cm^{-1}, respectively, in the spectrum. In addition, the two peaks at 2925 and 2854 cm^{-1} correspond to the asymmetric and symmetric stretching vibrations of the methylene group, respectively, which exist in the hydrolysate of APTES. The peaks at 3421, 2925, and 2854 cm^{-1} together verify that the silica-coated UCNPs have been successfully functionalized with amino groups.[34]

Characterization of Graphene Oxide and UCNPs-Go Complexes. The sample used for AFM examination was prepared by depositing a droplet of GO dispersion (3 μL, ∼20 μg·mL^{-1}) on a freshly cleaved mica surface and dried at room temperature. Figure S3 (Supporting Information) showed the typical AFM image of the prepared GO. From the depth profiles along the white line shown in Figure S3 (Supporting Information), it could be seen that the thickness of single-layer and bilayer GO was about 1.1 and 1.8 nm, respectively, which were also observed by other groups.[35] The absorption spectrum of GO (Figure 1d) spans a wide range of wavelengths (approximately 300−700 nm), overlapping the fluorescence spectra of $BaYF_5$:Yb Er/Tm UCNPs, in good accordance with literature results.[7] The formation of multicolor UCNPs-GO complex was verified with TEM and AFM (Figure S3, Supporting Information). The typical HRTEM image of as-prepared GO (Figure 2a) revealed that the GO sheet had occasional folds, wrinkles, and rolled edges. Multicolor UCNPs-GO complexes were formed by a π−π stacking effect between the nucleobases of aptamers and the sp^2 atoms of GO. The TEM image (Figure 2b) showed that many multicolor UCNPs were present on the GO sheets, which had characteristic wrinkles on the surface. It was indicated that multicolor UCNPs were brought close to the GO surface.

FRET between UCNPs and GO Induced by Aptamers. To confirm the fluorescence quenching was caused by aptamers-UCNPs-GO complexes, several control experiments were carried out. At 980 nm excitation, as shown in Figure 3a,

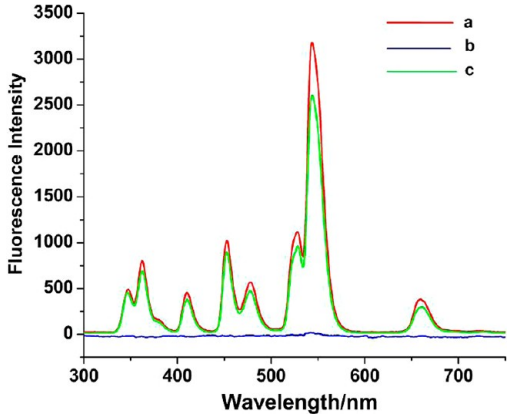

Figure 3. Upconversion fluorescence spectra of aptamers-$BaYF_5$:Yb Er/Tm UCNPs in Tris-HCl buffer before (a) and after (b) incubation with GO (0.6 mg·mL^{-1}) for 80 min; upconversion fluorescence spectra of amino-modified $BaYF_5$:Yb Er/Tm UCNPs in Tris-HCl buffer after addition of GO (0.6 mg·mL^{-1}) for 80 min (c). The concentrations of aptamers-UCNPs and amino-modified-UCNPs are both 0.5 mg·mL^{-1}.

aptamers-UCNPs exhibit intense upconversion fluorescence. However, the strong upconversion fluorescence of BaYF5:Yb Er/Tm can be completely quenched upon the addition of GO (Figure 3b). In contrast, the interaction between GO and free, unconjugated UCNPs results in only ∼23% fluorescence quenching (Figure 3c). The weak fluorescence quenching of pure UCNPs may be ascribed to the upconversion fluorescence being partly shielded by the black GO solution. As for aptamers-UCNPs, it has been documented that the aptamers-UCNPs can be brought in to close proximity to the GO surface through strong noncovalent π−π stacking interactions between the aptamers and GO. The results indicate that the absence or presence of aptamers is related to the highly efficient fluorescence quenching between aptamers-UCNPs and GO.

Effect of GO Concentration on the Upconversion Fluorescence Quenching Efficiency. When the concentration of aptamers-UCNPs was fixed, the quenching efficiency was strongly influenced by the GO concentration. As shown in

dx.doi.org/10.1021/ac301534w | Anal. Chem. 2012, 84, 6263−6270

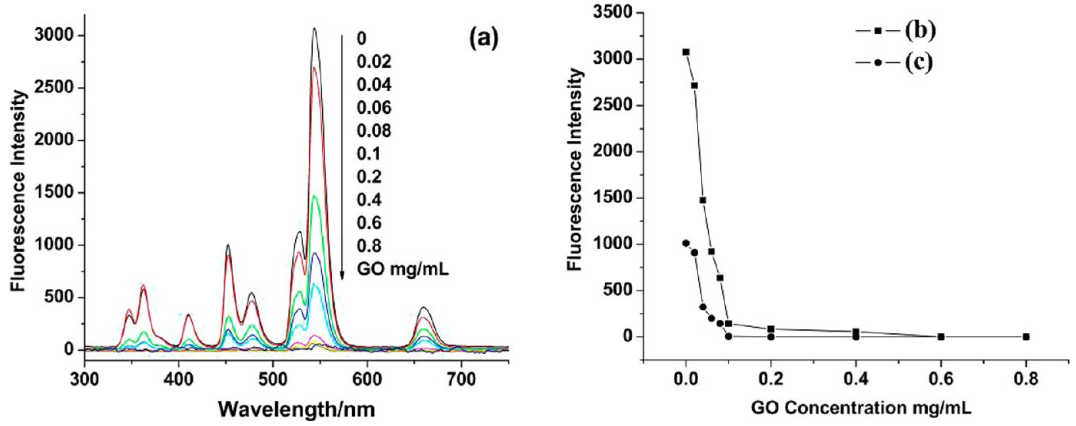

Figure 4. Upconversion fluorescence spectra of aptamers-$BaYF_5$:Yb Er/Tm-UCNPs (0.5 mg·mL^{-1}) after incubation with different concentrations of GO (a); the plot of $BaYF_5$:Yb Er fluorescence intensity recorded at 542 nm versus GO concentration (b) and the plot of $BaYF_5$:Yb Tm fluorescence intensity recorded at 452 nm versus GO concentration (c). The incubation of aptamers-$BaYF_5$:Yb Er/Tm-UCNPs and GO was carried out at 37 °C for 80 min.

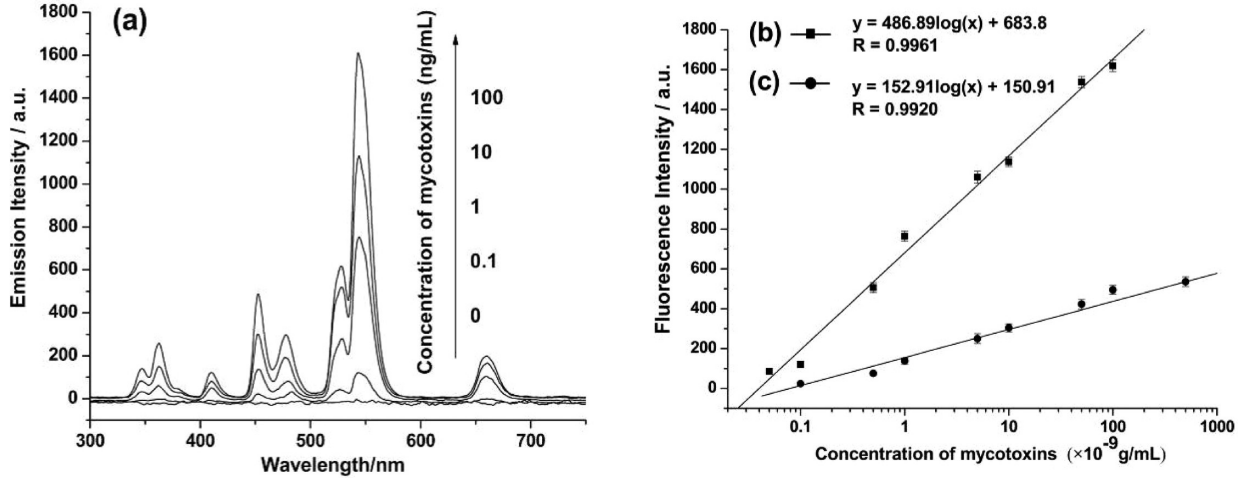

Figure 5. Upconversion fluorescence spectra of the multiplexed UCNPs-GO FRET aptasensor in the simultaneous presence of 0−100 ng·mL^{-1} FB_1 and OTA (a); standard curve of the fluorescence intensity versus OTA concentration (b) and FB_1 concentrations (c) measured by this developed method.

Figure 4, increasing the concentration of GO results in a decrease in the upconversion fluorescence intensity of OTA aptamers-$BaYF_5$:Yb Er UCNPs. Fluorescence tended to be completely quenched when GO concentration was higher than 0.6 mg·mL^{-1}. The fluorescence intensity of FB_1 aptamers-$BaYF_5$:Yb Tm UCNPs was quenched when the GO concentration exceeded 0.2 mg·mL^{-1}. The sensitivity of this upconversion fluorescence-enhanced detection assay was strongly dependent on the initial quenching efficiency of GO on UCNPs. Therefore, 0.6 mg·mL^{-1} GO was employed for high quenching efficiency of both types of $BaYF_5$ UCNPs.

Kinetic Characterization of the Upconversion Fluorescence Quenching Reaction. To study in depth the interactions between GO, aptamers-UCNPs, and the target mycotoxins (OTA and FB_1)-induced upconversion fluorescence recovery, time dependent fluorescence quenching experiments were conducted for aptamers-UCNPs and aptamers-UCNPs-target complexes in the presence of GO. As shown in Figure S4 (Supporting Information), when GO (0.6 mg·mL^{-1}) was added to OTA aptamers-$BaYF_5$:Yb Er solution, the upconversion fluorescence intensity showed immediate and rapid reduction and was completely quenched after 80 min. However, upon the addition of an equivalent GO, the OTA aptamers-$BaYF_5$:Yb Er solution displayed a slow decrease in the fluorescence intensity after 2 h of incubation with OTA (10 ng·mL^{-1}) at 37 °C. Even for 80 min, the fluorescence remained at ∼37% of the original intensity of OTA aptamers-$BaYF_5$:Yb Er in Tris-HCl buffer and remained stable for a further 2 h. Similarly, the fluorescence intensity of FB_1 aptamers-$BaYF_5$:Yb Tm UCNPs was completely quenched after 70 min by adding GO (0.6 mg·mL^{-1}) and incubating with FB_1 (10 ng·mL^{-1}); the fluorescence remained at ∼33% after addition of GO for 70 min. On the basis of these observations, an 80 min incubation time was selected for GO and aptamers-UCNPs or aptamers-UCNP-target mycotoxin complexes.

Multiplexed FRET Analysis of Target Mycotoxins. We chose to monitor the fluorescence of FB_1 and OTA at 452 and 542 nm, respectively, because the two emission peaks do not overlap at these wavelengths. In the absence of mycotoxin, the two groups' upconversion fluorescence of UCNPs would be completely quenched upon the addition of GO. In the presence of different concentrations of FB_1 and OTA, the gradual increase of upconversion fluorescence signals was observed with increasing concentrations of FB_1 and OTA (Figure 5a).

dx.doi.org/10.1021/ac301534w | Anal. Chem. 2012, 84, 6263−6270

Under optimal conditions, the concentration of mycotoxin was proportional to the increased fluorescence intensity (ΔI), wherein ΔI represented the difference of the upconversion fluorescence intensity excited by a 980 nm laser in the absence and in the presence of FB_1 or OTA. Figure 5b showed the linear relationship between the relative intensity of the upconversion fluorescence and the concentration of OTA. The linear range of this relationship varied from 0.05 ng·mL^{-1} to 0.1 μg·mL^{-1} (R = 0.9961). A good linear relationship was obtained between the fluorescence intensity and the concentration of FB_1 from 0.1 ng·mL^{-1} to 0.5 μg·mL^{-1} (R = 0.9920, Figure 5c). Statistical analysis revealed that the detection limit of FB_1 was 0.1 ng·mL^{-1} and OTA was 0.02 ng·mL^{-1}, as estimated with 3σ. The precision, expressed as the relative standard deviation (RSD) of OTA detection, was equal to 4.74% (1 ng·mL^{-1}, n = 7). The RSD of the FB_1 detection was equal to 5.86% (1 ng·mL^{-1}, n = 7), indicating that the developed method exhibited good reproducibility.

Specificity Evaluation and Analytical Application. Furthermore, aflatoxins B_1, B_2, G_1, and G_2 and fumonisin B_2 and zearalenone, which are homologues of other mycotoxins found in foods, can be evaluated by this same UCNPs-GO FRET-based method. The experimental results shown in Figure S5 (Supporting Information). indicate that only FB_1 and OTA induce a dramatic fluorescence enhancement at their corresponding peaks. The other analogues failed to generate significant fluorescence signals at the same concentrations, indicating that they cannot interact with aptamers to induce their structural conformation, which is likely due to the inherent specificity of the aptamers toward FB_1 and OTA.

The feasibility of applying the multiplexed FRET-based assay to measure FB_1 and OTA levels in naturally contaminated samples was validated using 15 specimens of maize obtained from local supermarkets. These specimens were measured by the developed method and a commercially available ELISA method. The results in Figure S6 (Supporting Information) showed that there is no significant difference between the two methods and that they are highly correlated (P < 0.0001). The accuracy of the measurements of FB_1 and OTA in agricultural commodities was also evaluated by determining the recovery of FB_1 and OTA by a standard addition method (where low, medium, and high levels of standard solution are added to the test solution). As shown in Table S1 (see Supporting Information), the recoveries of FB_1 were between 84.32% and 124.00%, and the recoveries of OTA were between 94.13% and 119.30%, indicating a high level of accuracy of the developed immunoassay. These analyses demonstrate that the proposed method can be applied to the analysis of FB_1 and OTA in real agricultural commodities.

CONCLUSION

In conclusion, we have constructed a novel sensor for the simultaneous determination of OTA and FB_1 using a multiplexed FRET from multicolor $BaYF_5$:Yb Er/Tm to graphene oxide. The multiplexed FRET system was first presented and used for analytical determinations. This novel pattern benefits from the optical features of UCNPs. They were excited by NIR light, suffered neither autofluorescence nor light scattering background, and the emission peaks of $BaYF_5$:Yb Er and $BaYF_5$:Yb Tm could be easily distinguished. More importantly, graphene oxide was an excellent energy acceptor because its absorption spectrum spans a wide range of wavelengths, overlapping with the fluorescence spectra of $BaYF_5$:Yb Er/Tm UCNPs. Hence, a multiplexed FRET system has been developed and applied to detect two types of mycotoxins simultaneously. Furthermore, our study has paved the way to wider applications for FRET systems: the energy donor and the energy acceptor of FRET were not only biunique but also multiple-to-one; thus, the multiplexed FRET-based detection can be used for various targets.

ASSOCIATED CONTENT

Supporting Information

Additional information as noted in text. This material is available free of charge via the Internet at http://pubs.acs.org.

AUTHOR INFORMATION

Corresponding Author

*Z.P.W.: e-mail, wangzp@jiangnan.edu.cn; tel/fax, +86-510-85917023. Q.Z.: e-mail, zhangqianlnu@gmail.com; tel/fax, +86-24-62202380.

Notes

The authors declare no competing financial interest.

ACKNOWLEDGMENTS

This work was partly supported by National S&T support program of China (2012BAK08B01), S&T Supporting Project of Jiangsu (BE2011621, BE2010679) and Guangdong (2011B0315000 25), Research Fund for the Doctoral Program of Higher Education (20110093110002), Doctor Candidate Foundation of Jiangnan University (10055), and NCET-11-0663.

REFERENCES

(1) Sapsford, K. E.; Berti, L.; Medintz, I. L. *Angew. Chem., Int. Ed.* **2006**, *45*, 4562−4588.
(2) Tsourkas, A.; Behlke, M. A.; Xu, Y. Q.; Bao, G. *Anal. Chem.* **2003**, *75*, 3697−3703.
(3) Zhou, D. J.; Piper, J. D.; Abell, C.; Klenerman, D.; Kang, D. J.; Ying, L. M. *Chem. Commun.* **2005**, *38*, 4807−4809.
(4) Wang, L. Y.; Yan, R. X.; Hao, Z. Y.; Wang, L.; Zeng, J. H.; Bao, H.; Wang, X.; Peng, Q.; Li, Y. D. *Angew. Chem., Int. Ed.* **2005**, *44*, 6054−6057.
(5) Cheng, L.; Yang, K.; Shao, M. W.; Lee, S. T.; Liu, Z. *J. Phys. Chem. C* **2011**, *115*, 2686−2692.
(6) Li, Z. Q.; Zhang, Y.; Jiang, S. *Adv. Mater.* **2008**, *20*, 4765−4769.
(7) Dong, H.; Gao, W.; Yan, F.; Ji, H.; Ju, H. *Anal. Chem.* **2010**, *82*, 5511−5517.
(8) Chang, H. X.; Tang, L. H.; Wang, Y.; Jiang, J. H.; Li, J. H. *Anal. Chem.* **2010**, *82*, 2341−2346.
(9) Liu, C. H.; Wang, Z.; Jia, H. X.; Li, Z. P. *Chem. Commun.* **2011**, *47*, 4661−4663.
(10) Zhang, C. L.; Yuan, Y. X.; Zhang, S. M.; Wang, Y. H.; Liu, Z. H. *Angew. Chem., Int. Ed.* **2011**, *50*, 6851−6854.
(11) Wang, Y. L.; Chai, T. J.; Lu, G. Z.; Quan, C. S.; Duan, H. Y.; Yao, M. L.; Zuckerc, B. A.; Schlenkerc, G. *Environ. Res.* **2008**, *107*, 139−144.
(12) Pamel, E. V.; Verbeken, A.; Vlaemynck, G.; Boever, J. D.; Daeseleire, E. *J. Agric. Food Chem.* **2011**, *59*, 9747−9755.
(13) Solfrizzo, M.; Gambacorta, L.; Lattanzio, V. M. T.; Powers, S.; Visconti, A. *Anal. Bioanal. Chem.* **2011**, *401*, 2831−2841.
(14) Corcueraa, L. A.; Ibáñez-Veab, M.; Vettorazzia, A.; González-Peñas, E.; Cerain, A. L. *J. Chromatogr., B* **2011**, *879*, 2733−2740.
(15) Rodríguez, A.; Rodríguez, M.; Andrade, M. J.; Córdoba, J. J. *Int. J. Food Microbiol.* **2012**, *155*, 10−18.
(16) Saha, K.; Agasti, S. S.; Kim, C. Y.; Li, X. N.; Rotello, V. M. *Chem. Rev.* **2012**, *112*, 2739−2779.

(17) Bonel, L.; Vidal, J. C.; Duato, P.; Castillo, J. R. *Biosens. Bioelectron.* **2011**, *26*, 3254−3259.
(18) Maka, A. C.; Osterfeldc, S. J.; Yu, H.; Wang, S. X.; Davis, R. W.; Jejelowod, O. A.; Pourmand, N. *Biosens. Bioelectron.* **2010**, *25*, 1635−1639.
(19) Hervás, M.; López, M. Á.; Escarpa, A. *Anal. Chim. Acta* **2009**, *653*, 167−172.
(20) Goldman, E. R.; Clapp, A. R.; Anderson, G. P.; Uyeda, H. T.; Mauro, J. M.; Medintz, I. L.; Mattoussi, H. *Anal. Chem.* **2004**, *76*, 684−688.
(21) Peng, C. F.; Li, Z. K.; Zhu, Y. Y.; Chen, W.; Yuan, Y.; Liu, L. Q.; Li, Q. S.; Xua, D. H.; Qiao, R. R.; Wang, L. B.; Zhu, S. F.; Jin, Z. Y.; Xu, C. L. *Biosens. Bioelectron.* **2009**, *24*, 3657−3622.
(22) Wu, S. J.; Duan, N.; Zhu, C. Q.; Ma, X. Y.; Wang, M.; Wang, Z. P. *Biosens. Bioelectron.* **2011**, *30*, 35−42.
(23) McKeague, M.; Bradley, C. R.; De Girolamo, A.; Visconti, A.; Miller, J. D.; DeRosa, M. C. *Int. J. Mol. Sci.* **2010**, *11*, 4864−4881.
(24) Cruz-Aguado, J. A.; Penner, G. *J. Agric. Food Chem.* **2008**, *56*, 10456−10461.
(25) Wu, S. J.; Duan, N.; Wang, Z. P.; Wang, H. X. *Analyst* **2011**, *136*, 2306−2314.
(26) Qiu, H. L.; Chen, G. Y.; Sun, L.; Hao, S. W.; Han, G.; Yang, C. H. *J. Mater. Chem.* **2011**, *21*, 17202−17208.
(27) Stöber, W.; Fink, A. *J. Colloid Interface Sci.* **1968**, *26*, 62−69.
(28) Li, Z. Q.; Zhang, Y. *Angew. Chem., Int. Ed.* **2006**, *45*, 7732−7735.
(29) Hummers, W. S.; Offeman, R. E. *J. Am. Chem. Soc.* **1958**, *80*, 1339.
(30) Wang, Y.; Li, Z.; Hu, D.; Lin, C. T.; Li, J.; Lin, Y. *J. Am. Chem. Soc.* **2010**, *132*, 9274−9276.
(31) Lu, C. H.; Li, J.; Lin, M. H.; Wang, Y. W.; Chen, X.; Chen, G. N. *Angew. Chem., Int. Ed.* **2010**, *49*, 8454−8457.
(32) Chen, X. P.; Zhang, Q. Y.; Yang, C. H.; Chen, D. D.; Zhao, C. *Spectrochim. Acta. Part A* **2009**, *7*, 441−445.
(33) Vetrone, F.; Mahalingam, V.; Capobianco, J. A. *Chem. Mater.* **2009**, *21*, 1847−1851.
(34) Wang, M.; Hou, W.; Mi, C. C.; Wang, W. X.; Xu, Z. R.; Teng, H. H.; Mao, C. B.; Xu, S. K. *Anal. Chem.* **2009**, *81*, 8783.
(35) Zhang, C. L.; Yuan, Y. X.; Zhang, S. M.; Wang, Y. H.; Liu, Z. H. *Angew. Chem., Int. Ed.* **2011**, *50*, 6851.